doi:10.1093/brain/awp079 Brain 2009: 132; 2139–2150 | 2139

BRAIN
A JOURNAL OF NEUROLOGY

Resonance in subthalamo-cortical circuits in Parkinson's disease

Alexandre Eusebio,[1,2] Alek Pogosyan,[1] Shouyan Wang,[3] Bruno Averbeck,[1] Louise Doyle Gaynor,[1] Stéphanie Cantiniaux,[2] Tatiana Witjas,[2] Patricia Limousin,[1,4] Jean-Philippe Azulay[2] and Peter Brown[1]

1 Sobell Department of Motor Neuroscience and Movement Disorders, Institute of Neurology, Queen Square, London, UK
2 Department of Neurology and Movement Disorders, Timone University Hospital, Marseille, France
3 Hearing and Balance Centre, Institute of Sound and Vibration Research, University of Southampton, UK
4 Unit of Functional Neurosurgery, Institute of Neurology, Queen Square, London, UK

Correspondence to: Peter Brown,
Sobell Department of Motor Neuroscience and Movement Disorders,
Institute of Neurology,
33 Queen Square,
London, WC1N 3BG, UK
E-mail: p.brown@ion.ucl.ac.uk

Neuronal activity within and across the cortex and basal ganglia is pathologically synchronized, particularly at ~20 Hz in patients with Parkinson's disease. Defining how activities in spatially distributed brain regions overtly synchronize in narrow frequency bands is critical for understanding disease processes like Parkinson's disease. To address this, we studied cortical responses to electrical stimulation of the subthalamic nucleus (STN) at various frequencies between 5 and 30 Hz in two cohorts of eight patients with Parkinson's disease from two different surgical centres. We found that evoked activity consisted of a series of diminishing waves with a peak latency of 21 ms for the first wave in the series. The cortical evoked potentials (cEPs) averaged in each group were well fitted by a damped oscillator function ($r \geqslant 0.9$, $P < 0.00001$). Fits suggested that the natural frequency of the subthalamo-cortical circuit was around 20 Hz. When the system was forced at this frequency by stimulation of the STN at 20 Hz, the undamped amplitude of the modelled cortical response increased relative to that with 5 Hz stimulation in both groups ($P \leqslant 0.005$), consistent with resonance. Restoration of dopaminergic input by treatment with levodopa increased the damping of oscillatory activity (as measured by the modelled damping factor) in both patient groups ($P \leqslant 0.001$). The increased damping would tend to limit resonance, as confirmed in simulations. Our results show that the basal ganglia–cortical network involving the STN has a tendency to resonate at ~20 Hz in Parkinsonian patients. This resonance phenomenon may underlie the propagation and amplification of activities synchronized around this frequency. Crucially, dopamine acts to increase damping and thereby limit resonance in this basal ganglia–cortical network.

Keywords: synchronization; basal ganglia; resonance; Parkinson's disease; deep brain stimulation

Abbreviations: cEP = cortical evoked potential; DBS = deep brain stimulation; MRI = magnetic resonance imaging; STN = subthalamic nucleus; UPDRS = Unified Parkinson's Disease Rating Scale

Introduction

Electrophysiological recordings in patients with Parkinson's disease and animal models of this disorder demonstrate an exaggerated and oscillatory synchronization of neuronal activity in the basal ganglia at frequencies below about 30 Hz (Rivlin-Etzion *et al*., 2006; Uhlhaas and Singer, 2006; Hammond *et al*., 2007). Such prominent synchronization is not seen in healthy animals and is

Received October 1, 2008. Revised March 2, 2009. Accepted March 4, 2009. Advance Access publication April 15, 2009

suppressed by treatment with the dopamine prodrug, levodopa, and by dopamine agonists, in tandem with an improvement in symptomatology. This has lead to the suggestion that pathological synchrony at low frequency is mechanistically linked to phenotypic features of Parkinson's disease, such as tremor, slowness of movement and stiffness, although this remains to be established (Rivlin-Etzion *et al*., 2006; Uhlhaas and Singer, 2006; Hammond *et al*., 2007).

In patients with Parkinson's disease, in whom most data comes from surgical implantation of the subthalamic nucleus (STN) or globus pallidus, pathological synchrony tends to occur at ~20 Hz (Brown *et al*., 2001; Cassidy *et al*., 2002; Williams *et al*., 2002; Priori *et al*., 2004; Alegre *et al*., 2005; Foffani *et al*., 2005; Kuhn *et al*., 2005; Alonso-Frech *et al*., 2006; Devos *et al*., 2006; Fogelson *et al*., 2006; Weinberger *et al*., 2006; Lalo *et al*., 2008; Steigerwald *et al*., 2008; Bronte-Stewart *et al*., 2009). More recently, it has become clear that excessive synchrony is a feature of the entire basal ganglia–cortical network in Parkinson's disease, with populations of neurons not only synchronizing their activity locally, but also across levels. Thus, there is coherent rhythmic activity both between nuclei in the basal ganglia (Brown *et al*., 2001; Cassidy *et al*., 2002; Goldberg *et al*., 2004; Foffani *et al*., 2005), and between these and cortical areas (Marsden *et al*., 2001; Williams *et al*., 2002; Sharott *et al*., 2005; Fogelson *et al*., 2006; Lalo *et al*., 2008). In particular, in patients with Parkinson's disease, there is strong coherence between activity in STN and the cortex centred around 20 Hz (Marsden *et al*., 2001; Williams *et al*., 2002; Fogelson *et al*., 2006; Lalo *et al*., 2008). Such synchronization at ~20 Hz has been associated with slowness of movement in both correlative (Brown and Williams, 2005; Kuhn *et al*., 2006b, 2008, 2009; Weinberger *et al*., 2006; Ray *et al*., 2008) and interventional (Fogelson *et al*., 2005*a*; Chen *et al*., 2007; Eusebio *et al*., 2008) studies. Even though a causal rather than epiphenomenal link between this pathological synchronization and motor impairment is by no means proven, synchronization at ~20 Hz therefore appears worthy of further investigation as it may provide insight into the pathophysiology of parkinsonism.

Here, we explore the mechanism of the strong coupling of oscillations at ~20 Hz across basal ganglia–thalamo–cortical circuits, and propose and test the hypothesis that dopaminergic hypoactivity in Parkinson's disease exposes a network resonance at ~20 Hz that favours the propagation of activity at this pathological frequency around basal ganglia–cortical loops in patients with Parkinson's disease. To this end, we studied the cortical response to STN stimulation in Parkinson's disease patients receiving therapeutic high frequency deep brain stimulation (DBS) through electrodes implanted in the STN.

Materials and Methods

Patients and surgery

Most recordings were performed in eight patients (eight males, mean age 58.0 years ± 3.0; mean disease duration 14.1 years ± 1.6) in London. Patients participated with written informed consent and the permission of the Joint Ethics Committee of the National Hospital for Neurology and Neurosurgery and the Institute of Neurology. However, we also repeated the main experiment in an independent population of eight similar Parkinson's disease patients (seven males, mean age 62.1 years ± 2.0; mean disease duration 12.8 years ± 1.5) recorded in Marseille. These patients participated with written informed consent and the permission of the local Ethics Committee (CPP Marseille 2). The clinical details of all patients are summarized in Supplementary Table 1. Implantation of bilateral STN DBS electrodes was performed in all subjects for treatment of Parkinson's disease at least 6 months prior to study (mean 29.9 months ± 3.6). The implanted pulse generator used was a Kinetra® (Medtronic Neurological Division, Minneapolis, USA). The DBS electrode used was model 3389 (Medtronic Neurological Division, Minneapolis, USA) with four platinum-iridium cylindrical surfaces (1.27 mm diameter and 1.5 mm length) and a centre-to-centre separation of 2 mm. Contact 0 was the most caudal and Contact 3 was the most rostral. The intended coordinates at the tip of Contact 0 were 10–12 mm from the midline, 0–2 mm behind the midcommissural point and 3–5 mm below the anterior commissural-posterior commissural line. For the patients operated in London, adjustments to the intended coordinates were made in accordance with the direct visualization of STN in individual stereotactic MRI (Hariz *et al*., 2003) and implantation performed under local anaesthesia. Correct placement of the DBS electrodes in the region of the STN was further supported by: (i) effective intra-operative macro-stimulation; (ii) immediate postoperative stereotactic T_2-weighted MRI compatible with the placement of at least one electrode contact in the STN region; (iii) significant improvement in UPDRS motor score during chronic DBS off medication (14.9 ± 2.5) compared with UPDRS off medication with stimulator switched off (44.8 ± 4.5; $P < 0.0001$, paired *t*-test). The patients operated in Marseille were implanted under light general anaesthesia as previously described (Witjas *et al*., 2004). Intended coordinates were adjusted according to the direct visualization of STN in stereotactic MRI performed under general anaesthesia. Correct placement of the DBS electrodes in the region of the STN was further supported by: (i) intra-operative micro-recordings (five electrodes on each side); (ii) intra-operative macro-stimulation for the detection of capsular spread; (iii) intra-operative stereotactic telemetric radioscopy and immediate post-operative CT-scan providing final coordinates of each contact; (iv) significant improvement in UPDRS motor score during chronic DBS off medication (11.5 ± 3.0) compared with UPDRS off medication with stimulator switched off (32.8 ± 3.2; $P < 0.0001$, paired *t*-test).

Protocol

Our aim was to artificially synchronize activity in the STN area at different frequencies and to follow changes in its propagation characteristics, as indicated by the amplitude of the cortical evoked potentials (cEPs). Previous studies have shown that DBS applied in the vicinity of the STN reliably induces a cEP with a peak latency of 20–25 ms predominantly over the sensorimotor cortex of Parkinson's disease patients and likely to reflect orthodromic activation of basal ganglia projections to the cortex (Baker *et al*., 2002; MacKinnon *et al*., 2005). Earlier potentials (<10 ms) occur, but may be more inconsistently observed, at least in part because of their obscuration by stimulation artefact. For example, MacKinnon *et al*. (2005) found these after stimulation of only 6 out of 14 electrodes. These early potentials may represent the effects of anti-dromic activation of the hyperdirect pathway (Ashby *et al*., 2001; Baker *et al*., 2002; MacKinnon *et al*., 2005). As we wanted to specifically test the transfer function of

pathways originating in the STN or passing as close to this nucleus as possible, we choose to stimulate those DBS contacts affording the best clinical response, even though the highest amplitude cEPs may often be obtained with DBS applied through more dorsal contacts (MacKinnon *et al*., 2005).

All 16 patients were assessed after overnight withdrawal of anti-parkinsonian medication. Fifteen of the patients (those in whom a significant cEP was found; see below) were also recorded during another experimental session after administration, in a dispersible form, of their morning levodopa-equivalent dose of medication or 200 mg of levodopa, whichever was the higher. Experimental sessions on and off medication were performed on separate days due to time constraints. In London, the two experimental sessions were separated by a mean of 47 ± 7 days and the ON-drug session always followed the OFF-drug session. In Marseille, the two experimental sessions took place on two consecutive days and the OFF-drug session followed the ON-drug in two patients. In the OFF-drug state, the stimulator was switched off for at least 20 min and basal OFF-drug OFF-stim UPDRS III scoring was performed. About 75% of the UPDRS III score decrease occurs within this time frame following discontinuation of DBS (Temperli *et al*., 2003). All patients had maximal clinical effect using monopolar DBS (the implanted pulse generator being the anode). However, in this configuration, the stimulus artefact prevents any analysis of the evoked potentials (MacKinnon *et al*., 2005). Accordingly, the stimulator was turned back on using a bipolar configuration and the voltage increased to 130% of the monopolar voltage by way of compensation (MacKinnon *et al*., 2005). There was no evidence of capsular spread during DBS, as determined by clinical examination. The negative contact was the one used by the patient in a monopolar configuration. The positive contact was chosen next to the negative one. When the active contact was between two other contacts, the positive contact producing the best clinical effect was utilized. The pairs of contacts chosen for all patients are summarized in Supplementary Table 1. In addition, postoperative MRI or CT-scan was consistent with placement of at least one of these two contacts in the STN region. The clinical effect was assessed using the UPDRS III score after 20 min of DBS using the patients' usual therapeutic stimulation frequency and pulse width. All patients improved their UPDRS III score by at least 30% (mean 50.6% ± 2.4 in London and 63.6% ± 6.6 in Marseille; $P \leqslant 0.0001$ for both, paired *t*-tests), consistent with stimulation of the local STN area.

The Kinetra® stimulator stimulates alternately both sides, producing an artefact at twice the frequency actually used. Therefore, to avoid this and any interaction of evoked potentials elicited at different times from the two hemispheres, only the side with the best clinical benefit of DBS (assessed by the UPDRS III score) was stimulated (nine right sides). The same side was stimulated in the OFF- and ON-drug conditions using the same DBS parameters. In both conditions, the stimulator was turned off for the other side. Efficacy of the levodopa administration in the ON-drug state was assessed using the UPDRS III score about 30 min after ingestion of levodopa with the stimulator ON with the usual therapeutic parameters in order to diminish the discomfort of the patients (ON-DBS ON-drug state). All patients felt at ''best ON'' and improved their UPDRS III score by at least 25% compared with the ON-DBS OFF-drug state (mean 52.3% ± 5.9 in London and 60.4% ± 8.4 in Marseille; $P \leqslant 0.005$ for both, paired *t*-tests) before the start of the recording in the ON-drug state. Moreover, eleven of them experienced peak-dose dyskinesias throughout the recording in the ON-drug state. The four patients who did not have dyskinesias were not usually prone to this kind of abnormal movement in the ON-drug state. The duration of the experiment (~90 min) was consistent with the duration of efficacy of the medication. On three occasions, however, an additional dose of 200 mg levodopa was administered to the patient as they subjectively felt the effect of the first dose of levodopa was wearing off, even though no significant deterioration of the UPDRS III score was noticed. We then waited 30 min before resuming the experiment.

A baseline recording without stimulation was performed first and then STN stimulated at 5, 10, 15, 20 and 30 Hz in London, and 5 and 20 Hz in Marseille. Stimulation frequencies were assessed in pseudo-randomized order across patients and patients were not informed of the stimulation frequency. The stimulation settings (i.e. contacts and parameters) used during the experiments are summarized in Supplementary Table 1. In order to diminish the duration of the experiments, we waited 5 min after changing between frequencies before recording since it has been previously shown that this short duration is sufficient to produce a practical steady state in Parkinsonian motor symptoms (Moro *et al*., 2002).

EEG recordings

Patients were comfortably seated in a chair during the whole experiment. In London, scalp EEG was recorded through 19 Ag/AgCl electrodes covering the scalp according to the 10:20 international system and referenced to linked ear electrodes. One additional electrode was used to record the stimulus artefact and was located either along the wire ipsilateral to the stimulated STN (close to the burr-hole or to the mastoid) or in the vicinity of the stimulator case, whichever produced the highest amplitude artefact. Signals were amplified and filtered (band-pass filter: 0.25–300 Hz) and sampled at 1500 Hz using a Brain Dynamics Analyzer® amplification system (St Petersburg, Russia) and custom-written software (developed by A.P.). In addition, the signal from the electrode recording the stimulus artefact was amplified and filtered (band-pass filter: 530–30 000 Hz) using a Digitimer®160 amplifier (Digitimer Ltd, Hertfordshire, UK) and processed through an amplitude discriminator (custom-made Schmitt trigger) that produced a timing pulse coincident with the peak of the artefact, so that both analogue and digital representations of the stimulus timing (artefact) were recorded. In Marseille, scalp EEG was recorded using 11 Ag/AgCl electrodes covering the sensorimotor cortex (Fp1, Fp2, F3, F4, Fz, C3, C4, Cz, P3, P4, Pz) referenced to linked ear electrodes. Signals were amplified and filtered (band-pass filter: 0.25–300 Hz) and sampled at 2048 Hz using a Porti® amplification system (TMS International, Oldenzaal, The Netherlands) and custom-written software (developed by A.P.). All recordings were performed at rest during 120 s after waiting 5 min between each frequency change.

Signal analysis

Recordings were edited using custom-made software (EditEEG©, developed by A.P.). Sections with artefacts from eye movements or scalp muscle activation were deleted. Recordings were then imported into Spike® version 2.06 (Cambridge Electronic Design, Cambridge, UK) using a custom-made script. The mean durations of the recordings in the OFF and ON conditions were 114.4 s ± 2.2 and 103.7 s ± 2.4 for 5 Hz, 115.0 s ± 2.3 and 99.6 s ± 3.2 for 10 Hz, 114.4 s ± 2.2 and 104.0 s ± 3.2 for 15 Hz, 113.8 s ± 3.0 and 107.2 s ± 3.4 for 20 Hz, 115.2 s ± 2.6 and 99.8 s ± 4.4 for 30 Hz for the patients from London (Group 1), and 80.4 s ± 3.6 and 86.0 s ± 8.1 for 5 Hz and 82.6 s ± 6.8 and 75.6 s ± 4.4 for 20 Hz for the patients from Marseille (Group 2). For each recording, channels were averaged around each artefact (trial width 0.4 s; offset 0.2 s) using Spike® version 2.06. The mean number of sweeps averaged in the OFF and

ON conditions were 578 ± 12 and 528 ± 13 for 5 Hz, 1123 ± 23 and 977 ± 32 for 10 Hz, 1697 ± 41 and 1553 ± 43 for 15 Hz, 2275 ± 60 and 2144 ± 69 for 20 Hz, 3428 ± 87 and 2993 ± 131 for 30 Hz for the patients from London (Group 1) and 402 ± 18 and 430 ± 41 for 5 Hz and 1652 ± 135 and 1512 ± 88 for 20 Hz for the patients from Marseille (Group 2). The recording lengths were slightly shorter in the ON-state compared with the OFF-state in the London group due to the presence of muscular artefacts caused by levodopa-induced dyskinesias, resulting in the deletion of larger sections of the recordings. Analysis of the averaged trials in the OFF-drug state showed that DBS consistently induced a significant cEP at 5 Hz with a peak latency of 18–25 ms in all but one patient (Case No. 8 in Supplementary Table 1), who was excluded from further analysis. The peak was considered significant when its amplitude exceeded 2 SD of the amplitude of the baseline trace (95% confidence limit) in at least one electrode over the sensorimotor cortex. The baseline trace was obtained by averaging the EEG recording in the OFF-drug state around fictitious events created in Spike® at 5 Hz when the stimulator was turned off (mean number of sweeps: 564 ± 13, not significantly different from the number of sweeps during genuine 5 Hz stimulation). The SD was measured for the 200 ms between each fictitious event. Short (3–8 ms) latency cEPs were not consistently seen, at least partly because of stimulation artefact. Cortical maps of the cEP amplitude averaged between 15 and 30 ms for all electrodes were created in Matlab® version 7.0.1 (The Mathworks Inc., Lowell, MA, USA) for the London patients and revealed maximum amplitudes over the sensorimotor, premotor and mesial cortices (Fig. 1). This was confirmed in an ANOVA of the cEP amplitude averaged between 15 and 30 ms for the ipsilateral, contralateral and mesial pairs of electrodes across the five different frequencies in both drug-states (3 levels × 5 levels × 2 levels). We found a significant effect of the pair of electrodes [$F(2,12) = 10.493$, $P = 0.002$] and within-subject contrasts revealed that the amplitude of the evoked potential was significantly higher for both mesial and ipsilateral electrodes compared with the contralateral electrodes across frequencies [$F(1,6) = 30.798$, $P = 0.001$ and $F(1,6) = 11.011$, $P = 0.016$, respectively; see Supplementary Fig. 1]. We thus analysed the cEPs in the corresponding electrodes (e.g. F3/F4, C3/C4, Fz, Cz) and decided accordingly to reduce the number of EEG electrodes in the Marseille patients. The peak latency of the first consistent cEP wave was measured for each patient (one side per patient) and at each stimulation frequency as the peak latency of the cEP averaged across these six electrodes between 15 and 30 ms. The cEPs were then averaged for each patient across the four electrodes covering the ipsilateral and mesial sensorimotor cortex obtained at different stimulation frequencies for further analyses. Similar cEPs were obtained with a fixed number of sweeps across stimulation frequencies instead of a fixed recording length (see Supplementary Fig. 2 and supplementary Table 2). We did not attempt a thorough source localization due to the relatively small number of electrodes used and the presence of burr holes.

Oscillation modelling

A free natural oscillation is damped if there is an external damping force to resist its changing and this was the model we choose to

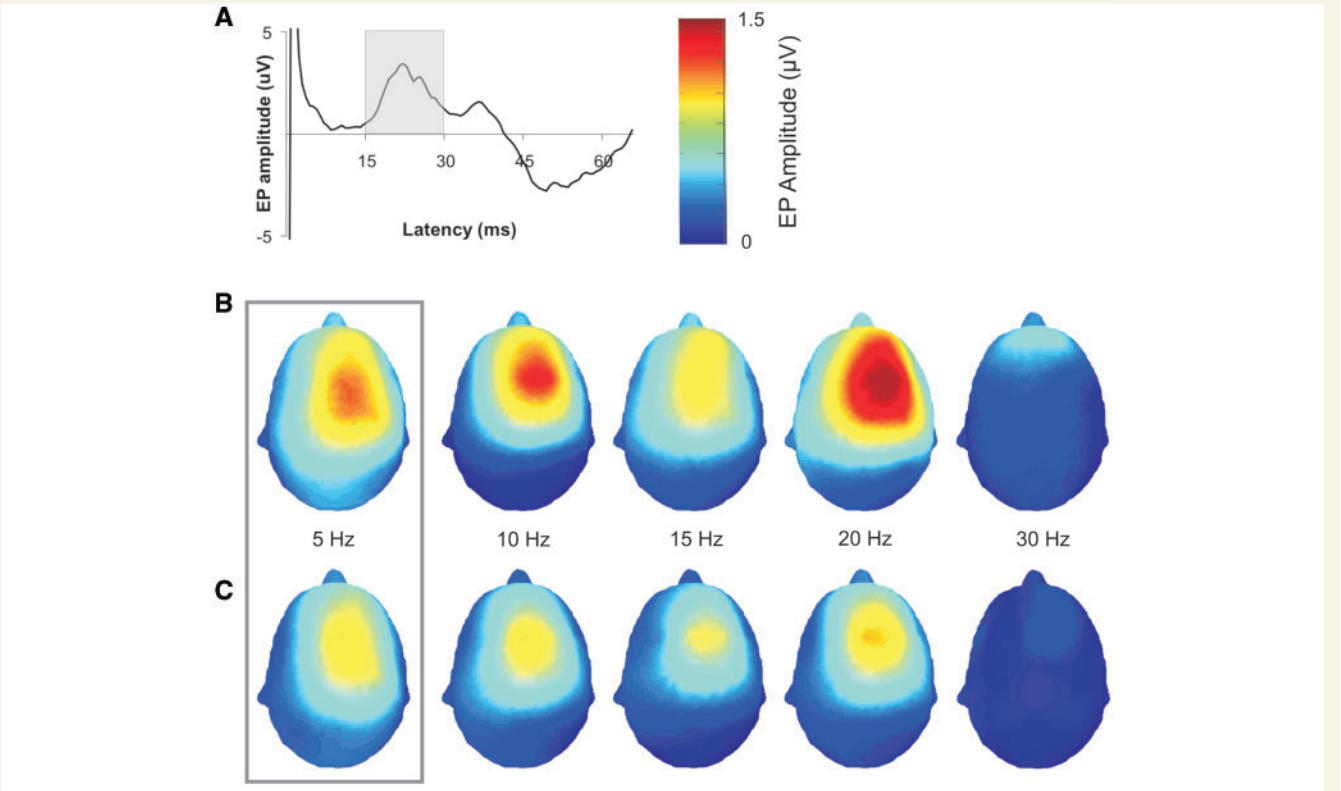

Figure 1 Shape and distribution of the cortical evoked potentials. (**A**) Example of cEP in Case 1 from Group 1 (see Supplementary Table 1) OFF-drug during 5 Hz stimulation. The time period over which cEP amplitude was averaged in B and C is indicated by the grey box. The initial portion of the trace (up to ~5 ms) is dominated by stimulation artefact. (**B** and **C**) Scalp maps of peak amplitudes of cEPs of 15–30 ms latency averaged across all seven patients in OFF-drug (**B**) and ON-drug (**C**) states for each stimulation frequency. Where necessary data were flipped so that scalp maps correspond to right hemisphere stimulation.

describe the cortical cEP (Pain, 2005; Rao, 1995). The damping oscillation can be described by a two-order differential equation as

$$m\ddot{x} + c\dot{x} + kx = 0 \quad (1)$$

where $x(t)$ is the damped oscillation, $\dot{x}$ and $\ddot{x}$ are first- and second-order differentiation of $x(t)$. Parameters m and k are the mass and elasticity constant. Parameter c is a damping constant, which is related to the level of damping force. Damping force is directly proportional to the changing of oscillation $x(t)$ as $F = -c\dot{x}$. If we define

$$\omega_n = \sqrt{\frac{k}{m}},\ \zeta = \frac{c}{2\sqrt{km}}$$

where ω_n is the natural frequency in radians of the undamped natural oscillation. ζ is a damping factor.

Then the damped oscillation $x(t)$ is expressed in the following function as the solution of Equation (1)

$$x(t) = X_0 e^{-\zeta\omega_n t}\cos\left(\sqrt{1-\zeta^2}\omega_n t - \phi_0\right) \quad (2)$$

ϕ_0 is the initial phase angle of the oscillation. X_0 is the amplitude of the natural oscillation.

When ζ is zero, the oscillation is a free natural oscillation without damping. When ζ is 1, the oscillation is critically damped and the solution of the Equation (1) becomes

$$x(t) = (X_0 + (\dot{x}(0) + \omega_n X_0)t)e^{-\omega_n t} \quad (3)$$

where $\dot{x}(0)$ is a constant of the initial value of $\dot{x}$.

As the recorded physiological signal usually has a floating baseline, we adjusted Equations (2) and (3) as

$$x(t) = X_0 e^{-\zeta\omega_n t}\cos\left(\sqrt{1-\zeta^2}\omega_n t - \phi_0\right) + \mathrm{A}t + \mathrm{D} \quad (4)$$

$$x(t) = (X_0 + (\dot{x}(0) + \omega_n X_0)t)e^{-\omega_n t} + \mathrm{A}t + \mathrm{D} \quad (5)$$

where $At + D$ represents the linear or constant floating baseline.

The parameters X_0, ω_n, ζ and ϕ_0 were estimated from the average evoked cortical potentials at 5, 10, 15, 20 and 30 Hz stimulation in Matlab® version 7.0.1 (The Mathworks Inc., Lowell, MA, USA). The stimulation artefacts were deleted from the ERP, to avoid the influences of artefacts on parameter estimation (See Supplementary Fig. 3). The processed ERP was then fitted with the waveform generated by Equation (3) according to the least mean square principle. The optimized parameters were iteratively computed till the mean square of the residual between the average ERP and fitting waveforms was minimal.

We only analysed data between stimulus artefacts over a single averaged stimulation cycle. This meant that stimulation artefact was not analysed but fewer data points were analysed for higher stimulation frequencies. However, qualitatively similar results were derived when several stimulation cycles of stimulation at 15–30 Hz were considered with the artefact deleted, so that similar numbers of data points were analysed across frequencies (data not shown). We first fitted the traces averaged across subjects for each stimulation frequency and both OFF- and ON-drug states. Wavelet transform filters were used to clean the average ERP as they provided reliable decomposition according to the waveform of short data segment. The data were low-pass filtered to remove EMG activity (London: 80–90 Hz for all stimulation frequencies, except for 30 Hz where a low pass of 135 Hz was used; Marseille: 110–120 Hz for both 5 and 20 Hz). In addition, a linear floating baseline for 5 Hz (constant baseline for all other frequencies) was incorporated in the model so as to correct for DC offsets.

Both cEPs averaged across groups (London and Marseille) and within patients were fitted using the above procedures. When analysing data from individual patients, the last 60 ms of the 200 ms cEP trace was deleted from one case from London and the last 90 ms was deleted in three cases from Marseille due to muscular artefacts. One case from London showed a natural frequency of 48 Hz, with a ~20 Hz component being identified in the residual to this fit. It was the results from the latter fit that were considered further as this lower frequency component appeared homologous to that seen in the remaining individual subjects in whom the predominant natural frequency was around 20 Hz. Note that harmonically related components may not merely reflect irregularities in waveform shape but can also be accompanied by multi-unit activity in resonant brain systems (Rager and Singer, 1998).

Finally, we simulated the response of an oscillating system with a natural frequency of 20 Hz and variable damping factors (0.05–0.6) when the system was driven by impulse input at frequencies from 1 to 60 Hz. The initial undamped amplitude was set as one and the peak amplitude relative to the initial value was extracted from the model for various stimulation frequencies and damping factors (Fig. 3).

Transfer function

The transfer function was estimated by fitting a convolution kernel which best predicted the EEG signal using the stimulus train. Specifically, we fit the following model:

$$y(t) = a + \sum_{k=0}^{n} h(k)s(t-k) + \eta \quad (6)$$

where $y(t)$ is the EEG signal, $h(k)$ is the convolution kernel, and $s(t-k)$ is the stimulus train and η is a Gaussian random variable. The convolution kernel was then estimated by minimizing the sum of the squared error (SSE) of the estimate of y

$$\mathrm{SSE} = \left(y(t) - \left(a + \sum_{k=o}^{n} h(k)s(t-k)\right)\right)^2 \quad (7)$$

using linear regression techniques. The frequency domain representation was then found by taking the Fourier transform of the convolution kernel, $h(k)$, with respect to k.

The transfer function, unlike the oscillation model, which operates on the average stimulus triggered cEP, controls for the fact that some stimuli arrive before the effects of the previous stimuli have gone to zero. More specifically, the transfer function controls for autocorrelation in the input stimulus. This is because the transfer function estimate, h, is equal to the cEP premultiplied by the inverse of the autocorrelation matrix of the stimulus. To see this, if we put the raw cEP data into a vector, y and the lagged stimulus values into a matrix S, we can write the solution of the vector of the convolution kernel as

$$h = (S^T S)^{-1} S^T y. \quad (8)$$

These are the normal equations from regression, i.e. they are the equations used to find the solution to the coefficients in multivariate regression (Draper and Smith, 1998). The matrix $S^T S$ is equivalent to the autocorrelation matrix of the stimulus train, and the vector $S^T y$ is equivalent to the average evoked potential. Thus, pre-multiplying by the inverse of $S^T S$ deconvolves the transfer function estimate. If the input stimulus were truly a delta function, or if it were white noise, this step would not be necessary. If the stimulus were white noise, the matrix $S^T S$ is a scaled identity matrix, and therefore it would

only scale the estimate of h, it would not change its frequency content.

Statistics

cEP amplitudes, latencies, fitted oscillator parameters (undamped amplitude, damping coefficient and natural frequency) and transfer function derived amplitudes were normally distributed (One-sample Kolmogorov Smirnov tests $P>0.05$). Repeated measures ANOVAs with repeated within-subjects contrasts were performed to compare the effects of drug-state and different frequencies of stimulation on cEP latencies and predominant cortical distribution. Mauchly's test was used to determine the sphericity of the data entered in the ANOVAs, and where data were non-spherical Greenhouse-Geisser corrections applied. Oscillator parameters were compared using two-tailed, paired Student's t-test (using step-wise correction for multiple comparisons). Means $\pm$SEM are presented throughout the text. All statistical analyses were performed in SPSS (SPSS for Windows version 12, SSPS Inc., Chicago, Illinois, USA).

Results

We stimulated the STN with trains of delta functions (pulses) at lower frequencies than used clinically in two groups of eight Parkinson's disease patients from different surgical centres, and contrasted the amplitudes of the potentials evoked in cortex (cEPs). We stimulated the STN only on the most severely affected side demonstrating the best clinical benefit to therapeutic stimulation.

Patient Group 1 (from London)

The natural frequency of the modelled STN-cortical circuit is about 20 Hz

A significant cEP (Fig. 1A) was observed in seven patients from this group during STN stimulation at 5 Hz. The peak latency of the first consistent wave of the cortical response was 21.2 ± 1.3 ms. Scalp mapping of the $\sim$21 ms component during 5 Hz stimulation indicated that cEP amplitude was maximal ipsilateral to the stimulated STN and over mesial cortical areas (see box in Fig. 1 where hemispheres have been reversed for right-sided stimulation prior to averaging, and Supplementary Fig. 1). Accordingly, we focused on the cEPs recorded through the four electrodes covering the ipsilateral and mesial sensorimotor cortex, averaging the cEPs at these sites in each patient. Averaged cEPs to STN stimulation at 5 Hz consisted of a series of diminishing waves with periods of around 50 ms (see box in Fig. 2A), consistent with the response of an impulse forced damped oscillator with a natural frequency of about 20 Hz. To test this, we fitted a damped oscillator function to the grand average of STN stimulation at 5 Hz according to the least mean squares principle. The fit was excellent ($r=0.9$, $P<0.00001$, box in Fig. 2A). The natural frequency of the damped oscillator fitting the cEP was 19.8 ± 0.1 Hz, the undamped amplitude (e.g. the theoretical amplitude of the response of the undamped system) $1.7\pm0.1\,\mu$V and the damping factor 0.14 ± 0.01.

Oscillatory responses are damped by dopaminergic therapy

We then recorded cEPs to 5 Hz STN stimulation in the same patients from Group 1 after treatment with levodopa was recommenced (hereafter referred to as ON-drug state). This drug helps restore dopaminergic tone in Parkinson's disease, and, as is usually the case, the motor state of our patients improved in the ON-drug state (see Materials and methods section). The pattern of the cEP was similar to that OFF-drug, with the exception that successive waves reduced in amplitude faster in the ON-drug state. The ON-drug state grand average cEP was again well fitted by a damped oscillator function ($r=0.9$, $P<0.00001$, box in Fig. 2A). The undamped amplitude was the same ($1.7\pm0.1\,\mu$V) and the natural frequency of the damped oscillator fitting the cEP slightly lower (18.1 ± 0.1 Hz) than that in the OFF-drug state. Importantly, however, and consistent with the observation that successive cEP waves reduced in amplitude faster after levodopa, the damping factor was $\sim$30% higher in the ON-drug state (0.18 ± 0.01, $P=0.001$).

The above findings were corroborated in individual subjects (Fig. 2C). A damped oscillator function was fitted to the average cEPs to STN stimulation at 5 Hz OFF- and ON-drug from each subject. Fits in all cases were good (mean $r=0.78\pm0.03$, range 0.51–0.95, $P<0.00001$). As above, the undamped amplitude did not differ between drug-states (2.1 ± 0.7 and $2.2\pm0.8\,\mu$V ON and OFF-drugs, respectively; $P=0.733$), and the natural frequency of the damped oscillator fitting the cEP was slightly lower ON- than OFF-drugs (20.7 ± 4.9 and 22.9 ± 4.4 Hz, respectively; $P=0.048$). The damping factor was 64% higher ON-drugs (0.18 ± 0.05) than OFF-drugs (0.11 ± 0.04; $P=0.001$).

Stimulation at 20 Hz provokes resonance and this resonant response is attenuated by dopaminergic therapy

The finding that the natural frequency of the modelled system underlying the cEP was $\sim$20 Hz encouraged us to seek evidence of resonance when this system was forced by stimulating the STN at 20 Hz. To this end, we stimulated STN at several additional frequencies in the patients from London (10, 15, 20 and 30 Hz), having first confirmed that the output current and waveform of the chronically implanted pattern generator used to stimulate patients remained constant across the different stimulation frequencies (See Supplementary Fig. 4). As before, we fitted damped oscillator functions to each grand average from stimulation at a given frequency for each drug state. Fits were very good ($r>0.94$, $P\leqslant0.00001$, Fig. 2A), confirming that the potentials evoked in cortex by STN stimulation were well described as the response of an impulse forced damped oscillator at all the frequencies of STN stimulation tested. Critically, the undamped amplitude of cEPs was clearly greatest during stimulation at 20 Hz ($3.1\pm0.7\,\mu$V at 20 Hz OFF versus $1.7\pm0.1\,\mu$V at 5 Hz OFF, $P=0.0053$ corrected for multiple comparisons; Fig. 2B). There was no difference in the undamped amplitudes between drug states during 20 Hz stimulation ($3.1\pm0.7\,\mu$V, both ON- and OFF-drug).

Simulation of the response of an oscillating system with a natural frequency of 20 Hz suggested that the changes in damping

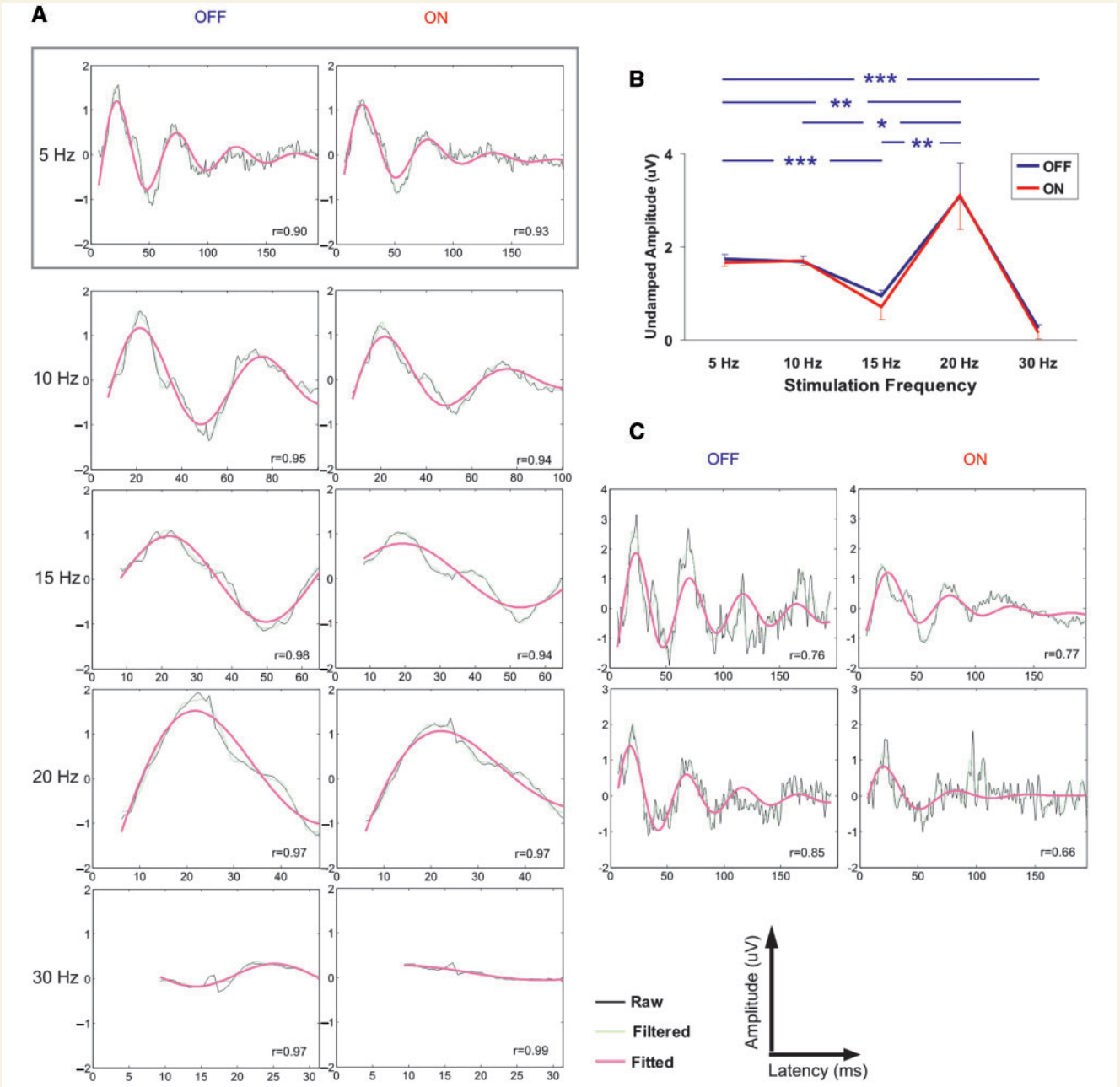

Figure 2 Fittings and parameters of the oscillator OFF- and ON-drugs. (**A**) Fitting of cEP traces averaged across seven patients in Group 1 in OFF- and ON-drug states for each stimulation frequency by the function for an impulse forced damped oscillator. Both the raw (black) and filtered (green) traces are indicated along with the fitted function (pink) (r = correlation coefficient for each fit). Stimulation artefacts at <5 ms latency are deleted for clarity. (**B**) Undamped amplitude in both drug states (P-values corrected for multiple comparisons: $*P<0.05$; $**P<0.005$; $***P<0.0001$) (**C**) Example fits in two Parkinson's disease patients (Cases 2 and 3) stimulated at 5 Hz.

factors identified between drug states in patients were sufficient to make a major difference to resonance phenomena (Fig. 3). Another relevant factor in this regard was the slight drop in natural frequency of the damped oscillator fitting the cEP with drug treatment noted above. This too would contribute to the reduction in observed resonance during driving at 20 Hz, although under natural conditions pure driving at 20 Hz is rather unlikely, as suggested by the breadth of activity in the beta frequency band in power spectra of STN local field potentials (Brown and Williams, 2005; Bronte-Stewart *et al*., 2008), so the effect of the drop in natural frequency upon resonance phenomena may not be as important as the increase in damping upon treatment. Note that the response to STN stimulation at 30 Hz did not merely recover after the resonance at 20 Hz, but was actually diminished relative

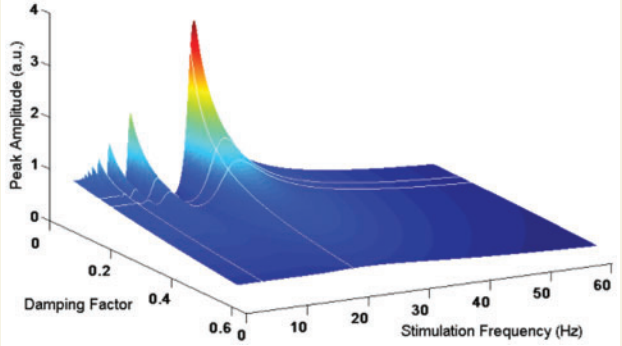

Figure 3 Simulation of response of an oscillating system with a natural frequency of 20 Hz showing dependency of resonance phenomena on damping factor. Changes in damping factor of the same degree as seen with the shift from the OFF- to ON-drug state, are sufficient to have a major effect on the amplitude of oscillations during stimulation at 20 Hz. Note there is a dip in amplitude with stimulation at 15 Hz that parallels the dip in undamped amplitude in Fig. 2B. White horizontal lines indicate a damping factor of 0.18 (ON) and 0.14 (OFF), as in patient Group 1, and vertical lines indicate 5 and 20 Hz stimulation.

to stimulation at 5 Hz, regardless of drug state (Figs. 1B and C; 2A and B). This suggested an additional low-pass filtering effect of the system underlying the cEP although proof of this would require stimulation at even higher frequencies.

In the above analysis, we assumed in our modelling that the responses of the impulse forced oscillator were unaffected by linear summation of the early evoked components to one pulse with the later evoked components of earlier pulses. This was not a factor when modelling the response to 5 Hz as Fig. 2A shows that the response had died off before the next stimulus. However, this may have been a factor with stimulation at 20 Hz, particularly in the OFF-drug state where the damping of successive oscillations was reduced. To investigate this point further we used an alternative approach involving the transfer function that modelled the effect of the most recent stimulus having allowed for the effect of earlier stimuli on the evoked activity in each subject. An ANOVA of FREQUENCY (5 levels: 5, 10, 15, 20 and 30 Hz) in the OFF-drug state confirmed an effect of frequency [$F(4,24) = 4.681$, $P = 0.006$] and within-subjects contrasts indicated that the response to 20 Hz stimulation was greater than that to 5 Hz stimulation [$F(1,6) = 7.308$, $P = 0.035$]. Thus, irrespective of any effect of linear summation, the response to an input at 20 Hz was bigger than that to an input at 5 Hz (See Supplementary Fig. 5).

The properties of the network change with dopamine and stimulation frequency but the network itself remains the same

Our core results suggested that basal ganglia–cortical circuits may have a natural oscillation frequency of about 20 Hz, that the amplitude of the cortical response to STN stimulation increases when the system is driven at or near its natural frequency and that this resonance phenomenon is predominantly limited by damping which is under the strong influence of dopaminergic input. This physiological interpretation assumes that the cortical response to STN stimulation at different frequencies and in different drug states has essentially the same mechanism. This assumption is supported by three observations. First, the same damped oscillator model fitted the grand average data well across stimulation conditions. Second, the latency of the initial wave in the cEP remained similar across conditions. Thus there was no significant effect of stimulation frequency, drug-state nor interaction between these two factors on the latencies of this wave as revealed by an ANOVA of latencies with factors FREQUENCY (5 levels: 5, 10, 15, 20 and 30 Hz) and STATE (two levels: OFF-drug and ON-drug). Third, the relative scalp topography (but not amplitude; Fig. 1B and C) of the cEP remained similar across conditions.

Patient Group 2 (from Marseille)

A natural frequency of about 20 Hz and increased damping with dopamine are consistent features

In order to determine the reproducibility of our core findings in patient Group 1 we repeated the experiment in an independent population of eight Parkinson's disease patients (Group 2) from a different surgical centre (Marseille). The cEPs were recorded during 5 Hz STN stimulation both in OFF- and ON-drug states. As before, the cEPs averaged over the ipsilateral and mesial sensorimotor cortex, consisted of a series of diminishing waves with a peak latency of 21.6 ± 0.6 ms for the first consistent wave. The fitted grand average cEP ($r = 0.9$ OFF and 0.95 ON, $P < 0.00001$, for both) had a natural frequency of 21.8 ± 0.1 Hz OFF and 20.8 ± 0.1 Hz ON ($P < 0.00001$) and a damping factor of 0.13 ± 0.01 OFF drugs increasing by 85% to 0.24 ± 0.01 ON-drugs ($P < 0.00001$; Fig. 4). As before the undamped amplitude of cEPs was greater during stimulation at 20 Hz (3.9 ± 0.3 μV at 20 Hz) than during 5 Hz stimulation OFF ($P = 0.002$; Fig. 4). The only major difference between this cohort of Parkinson's disease patients and those reported above was a higher undamped amplitude OFF (2.8 ± 0.1 μV; $P < 0.00001$ OFF Group 1 versus Group 2) that increased even further ON-drugs during 5 Hz stimulation (4.4 ± 0.2 μV; $P < 0.00001$ Group 2 OFF versus ON).

The above findings were corroborated in individual subjects. A damped oscillator function was fitted to the average cEPs to STN stimulation at 5 Hz OFF- and ON-drug from each subject. Fits in all cases were good (mean $r = 0.85 \pm 0.03$, range 0.66–0.95, $P < 0.00001$). As above, the damping factor significantly increased by 53% ON-drugs (0.26 ± 0.04) compared with OFF-drugs (0.17 ± 0.04; $P < 0.05$). The modelled natural frequency (20.2 ± 1.2 and 22.0 ± 1.1 ON- and OFF-drugs, respectively; $P = 0.19$) nor the modelled undamped amplitude (4.8 ± 0.7 μV and 3.5 ± 0.6 μV ON- and OFF-drugs, respectively; $P = 0.16$) were significantly different between drug-states. In summary, the natural frequency of about 20 Hz and the increased damping

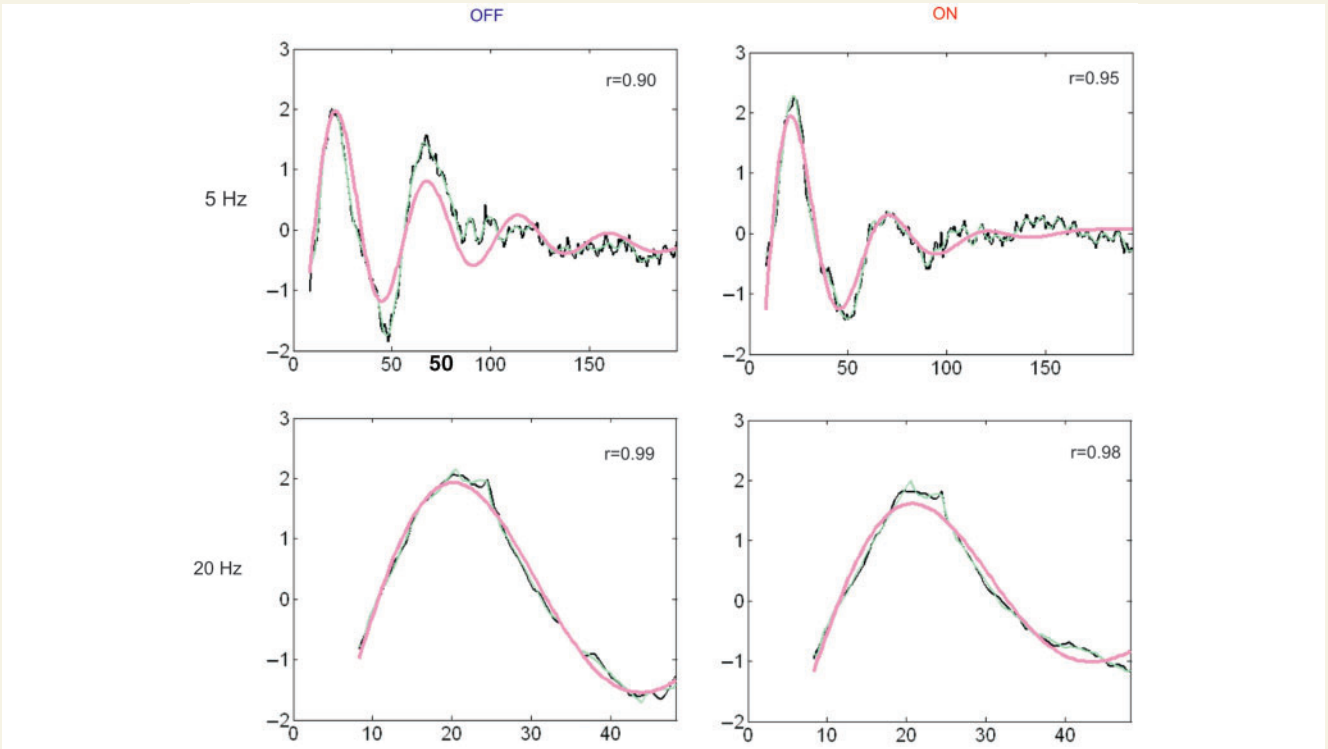

Figure 4 Fittings and parameters of the oscillator OFF- and ON-drugs in an independent Parkinson's disease patient group. Fitting of cEP traces averaged across eight patients in Group 2 in OFF- and ON-drug states for 5 and 20 Hz stimulation by the function for an impulse forced damped oscillator. Both the raw (black) and filtered (green) traces are indicated along with the fitted function (pink) (r = correlation coefficient for each fit). Stimulation artefacts at ~5 ms latency are deleted for clarity.

of the modelled oscillatory response after levodopa were consistent findings within and across the two patient groups.

Discussion

Our findings are compatible with a scheme in which, at the systems level, basal ganglia–cortical circuits can act as an oscillator, with a tendency to resonate at around 20 Hz. Ordinarily, dopaminergic input to the basal ganglia cortical system effectively increases the damping of oscillations, thereby limiting resonance phenomena in these circuits. However, in the relative absence of dopaminergic input in the untreated Parkinson's disease patient the system becomes less damped and thus, resonance is more marked, contributing to the relatively preferential propagation and amplification of activities synchronized around 20 Hz. Our study focused on the dynamic response of basal ganglia–cortical circuits over five to 30 Hz, in line with the evidence for exaggerated and distributed oscillation at similar frequencies in the basal ganglia–cortical system of patients with Parkinson's Disease demonstrated by multiple groups (Brown *et al*., 2001; Cassidy *et al*., 2002; Williams *et al*., 2002; Priori *et al*., 2004; Alegre *et al*., 2005; Foffani *et al*., 2005; Kuhn *et al*., 2005; Alonso-Frech *et al*., 2006; Devos *et al*., 2006; Fogelson *et al*., 2006; Weinberger *et al*., 2006; Lalo *et al*., 2008; Steigerwald *et al*., 2008; Bronte-Stewart *et al*., 2009). However, as such we cannot exclude additional resonances at other frequencies, such as that reported in the cerebral cortex at frequencies around or above 100 Hz during DBS (Li *et al*., 2007; Montgomery and Gale, 2008).

The above interpretation of our findings makes no assumption regarding the site or sites within the circuit responsible for the oscillatory response. Although evident in the cEP, the resonance at ~20 Hz could have been partially or entirely generated at a subcortical relay and activity then propagated to the cortex. However, independent estimates of the preferred frequency response of circuits involving frontal and sensorimotor cortical areas generally also implicate frequencies of about 20 Hz. Thus, the natural frequency of the damped oscillator fitting the evoked responses corresponds closely to the frequency of steady state sensorimotor cortical responses to peripheral vibration (Tobimatsu *et al*., 1999), the predominant frequency of cortico-muscular coherence (Gilbertson *et al*., 2005) and the predilection of cortical myoclonus to occur at around 20 Hz (Ugawa *et al*., 2003).

A related issue is the nature of the pathway activated by STN stimulation that eventually modulates cortical activity. Previous reports suggest that the initial cEP wave peaking at ~21 ms is the product of activity in the subthalamo–pallidal–thalamo–cortical pathway (MacKinnon *et al*., 2005; Tisch *et al*., 2008), in line with recent animal work suggesting that regular trains of inhibitory pallidal discharges can drive phase-locked thalamocortical output, and hence produce a cEP (Person and Perkel, 2005). Furthermore, there is no evidence to indicate that later evoked waves might have a different origin in a system that is known to be

characterized by rhythmic activity at ~20 Hz (Brown *et al*., 2001; Rivlin-Etzion *et al*., 2006). Recent data, however, suggest the existence of direct subthalamo–cortical projections (Degos *et al*., 2008) and a fast orthodromic transmission followed by recruitment of cortico-cortical or cortico–subcortico–cortical loops cannot be excluded. Similarly, anti-dromic stimulation of the cortex via the hyperdirect pathway is possible, although this is generally believed to lead to initial activation of the cortex at latencies of under 10 ms (Ashby *et al*., 2001; Baker et al *et al*., 2002; MacKinnon *et al*., 2005), rather than 21 ms as in our recordings.

On the other hand, the nature of the pathway or pathways involved in the generation of the cEP oscillation does not necessarily impact on the functional significance of our findings as, irrespective of the pathways involved, the net effect at the cortical level is the preferential propagation of activities at around 20 Hz in untreated Parkinson's disease. The precise mechanisms by which restoration of dopaminergic input can modify the damping of oscillations and attenuate expression of 20 Hz activity at the cortical level remain unclear. One possibility is that dopamine alters voltage-dependent conductances (Nicola *et al*., 2000) that may act to dampen oscillations (Gutfreund *et al*., 1995). Alternatively, dopamine may alter potential re-entrant mechanisms in the basal ganglia–thalamo–cortical loop (Montgomery and Gale, 2008).

It is interesting to note that the natural frequency of around 20 Hz identified here is paralleled by the pattern of STN-cortical coherence in previous studies (Williams *et al*., 2002; Fogelson *et al*., 2006; Lalo *et al*., 2008). This suggests that the network properties characterized here may be of functional relevance in the amplification and propagation of spontaneous pathological oscillations in Parkinson's disease patients. However, further studies are required in peri-operative patients to determine whether the modelled natural frequency in each subject corresponds to the peak frequency of their STN-cortical coherence. The latter would be preferable to comparison with the peak frequency of their motor cortical EEG activity in the beta band, which may reflect synchronization supported not only by the basal ganglia, but also by cortico–cortical interactions and cerebello–thalamo–cortical relays (Marsden *et al*., 2000).

Another feature of note was that the response to STN stimulation at 30 Hz did not merely recover after the resonance at 20 Hz, but was actually diminished relative to stimulation at 5 Hz, regardless of drug state. This might reflect low-pass filtering by the skull and scalp and/or an additional low-pass filtering effect of the system underlying the cEP, consistent with a polysynaptic subthalamo–pallidal–thalamo–cortical relay, as frequency following in polysynaptic circuits tends to fail at higher frequencies. This might help explain why coherence between basal ganglia sites and cortex at frequencies in the gamma band is unusual, even though local field potentials power in the STN often has a discrete gamma band peak in treated patients (Marsden *et al*., 2001; Williams *et al*., 2002; Alegre *et al*., 2005; Fogelson *et al*., 2005*b*; Alonso-Frech *et al*., 2006; Devos *et al*., 2006), contrasting with the stereotypical coherence between basal ganglia sites and cortex in the beta band in patients with Parkinson's disease (Marsden *et al*., 2001; Williams *et al*., 2002; Fogelson *et al*., 2006; Kuhn *et al*., 2006*a*).

Finally, it is interesting to note that the natural frequency of around 20 Hz measured in our patients corresponds to the frequency band associated with slowness of movement in both correlative (Brown and Williams, 2005; Kuhn *et al*., 2006*b*, 2008, 2009; Weinberger *et al*., 2006; Ray *et al*., 2008) and interventional (Fogelson *et al*., 2005*a*; Chen *et al*., 2007; Eusebio *et al*., 2008) studies of STN. In the latter case there is evidence for impairment in motor function during stimulation of STN at around 20 Hz, but not at 15 or 30 Hz, when stimulation is performed in Parkinson's disease patients withdrawn from medication (Fogelson *et al*., 2005; Chen *et al*., 2007; Eusebio *et al*., 2008). This parallels the pattern of modelled resonance shown here. Indeed, stimulation at 40 and at 60 Hz is believed to improve some aspects of parkinsonism (Moreau *et al*., 2008; Brozova *et al*., 2009), as well as of dystonia and chorea (Moro *et al*., 2004; Alterman *et al*., 2007; Guehl *et al*., 2007). Likewise, our study provided evidence of a smaller tendency to resonance in the evoked response to stimulation of the STN at 10 Hz, evident in both the scalp topography of the cortical response at about 20 ms and in our simulations. It may be relevant, therefore, that exacerbations of motor impairment may also be seen with 10 Hz stimulation of the STN (Timmermann *et al*., 2004), although the same group has highlighted that this effect may be reversed when some cognitive functions are considered (Wojtecki *et al*., 2006), and the above observations may not apply to all targets for DBS in movement disorders. Thus stimulation of the region of the pedunculopontine nucleus at about 20 Hz is therapeutic (Lim *et al*., 2007; Stefani *et al*., 2007). Taken together these observations suggest that there may be several basal ganglia–cortical networks subserving different aspects of impairment in Parkinson's disease and each with its own pattern of susceptibility to resonance phenomena (Fogelson *et al*., 2006). Of these, the motor circuit involving STN may be particularly susceptible to frequencies of around 20 Hz, at least when dopaminergic activity is low.

In summary, the data presented here help explain why excessive neuronal synchrony at around 20 Hz in patients with Parkinson's disease is so remarkably propagated around the basal ganglia–cortical circuit involving the STN, leading to coherent activity over multiple levels within this circuit. The results show that this basal ganglia–cortical network has a tendency to resonate at ~20 Hz, thereby both propagating and amplifying spontaneous pathological activities at this frequency. Critically, dopamine acts to increase damping and thereby limit resonance in this basal ganglia–cortical network.

Supplementary material

Supplementary material is available at *Brain* online.

Acknowledgements

We thank Peter Magill, Pierre Pollak, Peter Redgrave, Stephen Tisch and Paul Sauleau for helpful comments, Vladimir Litvak for

help building scalp map plots, Jean-Claude Péragut and Jean Régis for operating on the Marseille patients and Marwan Hariz for operating on the London patients and proof-reading the manuscript.

Funding

Medical Research Council, Wellcome Trust, Parkinson Appeal (UK); Société Française de Neurologie—Journées de Neurologie de Langue Française (France).

References

Alegre M, Alonso-Frech F, Rodriguez-Oroz MC, Guridi J, Zamarbide I, Valencia M, et al. Movement-related changes in oscillatory activity in the human subthalamic nucleus: ipsilateral vs. contralateral movements. Eur J Neurosci 2005; 22: 2315–24.

Alonso-Frech F, Zamarbide I, Alegre M, Rodriguez-Oroz MC, Guridi J, Manrique M, et al. Slow oscillatory activity and levodopa-induced dyskinesias in Parkinson. Brain 2006; 129: 1748–57.

Alterman RL, Miravite J, Weisz D, Shils JL, Bressman S, Tagliati M. Sixty hertz pallidal DBS for primary torsion dystonia. Neurology 2007; 69: 681–98.

Ashby P, Paradiso G, Saint-Cyr JA, Chen R, Lang AE, Lozano AM. Potentials recorded at the scalp by stimulation near the human subthalamic nucleus. Clin Neurophysiol 2001; 112: 431–7.

Baker KB, Montgomery EB Jr, Rezai AR, Burgess R, Luders HO. Subthalamic nucleus deep brain stimulus evoked potentials: physiological and therapeutic implications. Mov Disord 2002; 17: 969–83.

Bronte-Stewart H, Barberini C, Koop MM, Hill BC, Henderson JM, Wingeier B. The STN beta-band profile in Parkinson's disease is stationary and shows prolonged attenuation after deep brain stimulation. Exp Neurol 2009; 215: 20–8.

Brown P, Oliviero A, Mazzone P, Insola A, Tonali P, Di Lazzaro V. Dopamine dependency of oscillations between subthalamic nucleus and pallidum in Parkinson's disease. J Neurosci 2001; 21: 1033–8.

Brown P, Williams D. Basal ganglia local field potential activity: character and functional significance in the human. Clin Neurophysiol 2005; 116: 2510–9.

Brozova H, Barnaure I, Alterman RL, Tagliati M. STN-DBS frequency effects on freezing of gait in advanced Parkinson disease. Neurology 2009; 72: 770.

Cassidy M, Mazzone P, Oliviero A, Insola A, Tonali P, Di Lazzaro V, et al. Movement-related changes in synchronization in the human basal ganglia. Brain 2002; 125: 1235–46.

Chen CC, Litvak V, Gilbertson T, Kuhn A, Lu CS, Lee ST, et al. Excessive synchronization of basal ganglia neurons at 20 Hz slows movement in Parkinson. Exp Neurol 2007; 205: 214–21.

Degos B, Deniau JM, Le Cam J, Mailly P, Maurice N. Evidence for a direct subthalamo-cortical loop circuit in the rat. Eur J Neurosci 2008; 27: 2599–610.

Devos D, Szurhaj W, Reyns N, Labyt E, Houdayer E, Bourriez JL, et al. Predominance of the contralateral movement-related activity in the subthalamo-cortical loop. Clin Neurophysiol 2006; 117: 2315–27.

Draper NR, Smith H. Applied regression analysis. New York: Wiley; 1998..

Eusebio A, Chen CC, Lu CS, Lee ST, Tsai CH, Limousin P, et al. Effects of low-frequency stimulation of the subthalamic nucleus on movement in Parkinson's disease. Exp Neurol 2008; 209: 125–30.

Foffani G, Ardolino G, Meda B, Egidi M, Rampini P, Caputo E, et al. Altered subthalamo-pallidal synchronisation in parkinsonian dyskinesias. J Neurol Neurosurg Psychiatry 2005; 76: 426–8.

Fogelson N, Kuhn AA, Silberstein P, Limousin PD, Hariz M, Trottenberg T, et al. Frequency dependent effects of subthalamic nucleus stimulation in Parkinson's disease. Neurosci Lett 2005a; 382: 5–9.

Fogelson N, Pogosyan A, Kuhn AA, Kupsch A, van Bruggen G, Speelman H, et al. Reciprocal interactions between oscillatory activities of different frequencies in the subthalamic region of patients with Parkinson's disease. Eur J Neurosci 2005b; 22: 257–66.

Fogelson N, Williams D, Tijssen M, van Bruggen G, Speelman H, Brown P. Different functional loops between cerebral cortex and the subthalmic area in Parkinson. Cereb Cortex 2006; 16: 64–75.

Gilbertson T, Lalo E, Doyle L, Di Lazzaro V, Cioni B, Brown P. Existing motor state is favored at the expense of new movement during 13–35 Hz oscillatory synchrony in the human corticospinal system. J Neurosci 2005; 25: 7771–9.

Goldberg JA, Rokni U, Boraud T, Vaadia E, Bergman H. Spike synchronization in the cortex/basal-ganglia networks of Parkinsonian primates reflects global dynamics of the local field potentials. J Neurosci 2004; 24: 6003–10.

Guehl D, Cuny E, Tison F, Benazzouz A, Bardinet E, Sibon Y, et al. Deep brain pallidal stimulation for movement disorders in neuroacanthocytosis. Neurology 2007; 68: 160–1.

Gutfreund Y, Yarom Y, Segev I. Subthreshold oscillations and resonant frequency in guinea-pig cortical neurons: physiology and modelling. J Physiol 1995; 483: 621–40.

Hammond C, Bergman H, Brown P. Pathological synchronization in Parkinson's disease: networks, models and treatments. Trends Neurosci 2007; 30: 357–64.

Hariz MI, Krack P, Melvill R, Jorgensen JV, Hamel W, Hirabayashi H, et al. A quick and universal method for stereotactic visualization of the subthalamic nucleus before and after implantation of deep brain stimulation electrodes. Stereotact Funct Neurosurg 2003; 80: 96–101.

Kuhn AA, Doyle L, Pogosyan A, Yarrow K, Kupsch A, Schneider GH, et al. Modulation of beta oscillations in the subthalamic area during motor imagery in Parkinson's disease. Brain 2006a; 129: 695–706.

Kuhn AA, Kempf F, Brucke C, Gaynor Doyle L, Martinez-Torres I, Pogosyan A, *et al*. High-frequency stimulation of the subthalamic nucleus suppresses oscillatory beta activity in patients with Parkinson's disease in parallel with improvement in motor performance. J Neurosci 2008; 28: 6165–73.

Kuhn AA, Kupsch A, Schneider GH, Brown P. Reduction in subthalamic 8–35 Hz oscillatory activity correlates with clinical improvement in Parkinson's disease. Eur J Neurosci 2006b; 23: 1956–60.

Kuhn AA, Trottenberg T, Kivi A, Kupsch A, Schneider GH, Brown P. The relationship between local field potential and neuronal discharge in the subthalamic nucleus of patients with Parkinson's disease. Exp Neurol 2005; 194: 212–20.

Kühn AA, Tsui A, Aziz T, Ray N, Brücke C, Kupsch A, et al. Pathological synchronisation in the subthalamic nucleus of patients with Parkinson. Exp Neurol 2009; 215: 380–7.

Lalo E, Thobois S, Sharott A, Polo G, Mertens P, Pogosyan A, et al. Patterns of bidirectional communication between cortex and basal ganglia during movement in patients with Parkinson disease. J Neurosci 2008; 28: 3008–16.

Li S, Arbuthnott GW, Jutras MJ, Goldberg JA, Jaeger D. Resonant antidromic cortical circuit activation as a consequence of high-frequency subthalamic deep-brain stimulation. J Neurophysiol 2007; 98: 3525–37.

Lim AS, Lozano AM, Moro E, Hamani C, Hutchison WD, Dostrovsky JO, et al. Characterization of REM-sleep associated ponto-geniculo-occipital waves in the human pons. Sleep 2007; 30: 823–27.

MacKinnon CD, Webb RM, Silberstein P, Tisch S, Asselman P, Limousin P, et al. Stimulation through electrodes implanted near the subthalamic nucleus activates projections to motor areas of cerebral cortex in patients with Parkinson's disease. Eur J Neurosci 2005; 21: 1394–402.

Marsden JF, Ashby P, Limousin-Dowsey P, Rothwell JC, Brown P. Coherence between cerebellar thalamus, cortex and muscle in man: cerebellar thalamus interactions. Brain 2000; 123 (Pt 7): 1459–70.

Marsden JF, Limousin-Dowsey P, Ashby P, Pollak P, Brown P. Subthalamic nucleus, sensorimotor cortex and muscle interrelationships in Parkinson's disease. Brain 2001; 124: 378–88.

Montgomery EB, Gale GT. Mechanisms of action of deep brain stimulation (DBS). Neurosci Biobehav Rev 2008; 32: 388–407.

Moreau C, Defebvre L, Destée A, Bleuse S, Clement F, Blatt JL, et al. STN-DBS frequency effects on freezing of gait in advanced Parkinson disease. Neurology 2008; 71: 80–4.

Moro E, Esselink RJ, Xie J, Hommel M, Benabid AL, Pollak P. The impact on Parkinson's disease of electrical parameter settings in STN stimulation. Neurology 2002; 59: 706–13.

Moro E, Lang AE, Strafella AP, Poon YY, Arango PM, Dagher A, et al. Bilateral globus pallidus stimulation for Huntington's disease. Ann Neurol 2004; 56: 290–4.

Nicola SM, Surmeier J, Malenka RC. Dopaminergic modulation of neuronal excitability in the striatum and nucleus accumbens. Annu Rev Neuwrosci 2000; 23: 185–215.

Pain HJ. Damped simple harmonic motion. The physics of vibrations and waves. Chichester, New York: Wiley; 2005. pp. 37–52.

Person AL, Perkel DJ. Unitary IPSPs drive precise thalamic spiking in a circuit required for learning. Neuron 2005; 46: 129–40.

Priori A, Foffani G, Pesenti A, Tamma F, Bianchi AM, Pellegrini M, et al. Rhythm-specific pharmacological modulation of subthalamic activity in Parkinson's disease is associated with improvements in bradykinesia after dopamine and deep brain stimulation. Exp Neurol 2004; 189: 369–79.

Rager G, Singer W. The response of cat visual cortex to flicker stimuli of variable frequency. Eur J Neurosci 1998; 10: 1856–77.

Rao SS. Mechanical vibrations. Reading, MA: Addison-Wesley; 1995.

Ray NJ, Jenkinson N, Wang S, Holland P, Brittain JS, Joint C, et al. Local field potential beta activity in the subthalamic nucleus of patients with Parkinson's disease is associated with improvements in bradykinesia after dopamine and deep brain stimulation. Exp Neurol 2008; 213: 108–13.

Rivlin-Etzion M, Marmor O, Heimer G, Raz A, Nini A, Bergman H. Basal ganglia oscillations and pathophysiology of movement disorders. Curr Opin Neurobiol 2006; 16: 629–37.

Sharott A, Magill PJ, Bolam JP, Brown P. Directional analysis of coherent oscillatory field potentials in the cerebral cortex and basal ganglia of the rat. J Physiol 2005; 562: 951–63.

Stefani A, Lozano AM, Peppe A, Stanzione P, Galati S, Tropepi D, et al. Bilateral deep brain stimulation of the pedunculopontine and subthalamic nuclei in severe Parkinson's disease. Brain 2007; 130: 1596–607.

Steigerwald F, Potter M, Herzog J, Pinsker M, Kopper F, Mehdorn HM, et al. Neuronal activity of the human subthalamic nucleus in the Parkinsonian and non-Parkinsonian state. J Neurophysiol 2008; 100: 2515–24.

Temperli P, Ghika J, Villemure JG, Burkhard PR, Bogousslavsky J, Vingerhoets FJ. How do parkinsonian signs return after discontinuation of subthalamic DBS? Neurology 2003; 60: 78–81.

Timmermann L, Wojtecki L, Gross J, Lehrke R, Voges J, Maarouf M, et al. Ten-Hertz stimulation of subthalamic nucleus deteriorates motor symptoms in Parkinson's disease. Mov Disord 2004; 19: 1328–33.

Tisch S, Rothwell JC, Zrinzo L, Bhatia KP, Hariz M, Limousin P. Cortical evoked potentials from pallidal stimulation in patients with primary generalized dystonia. Mov Disord 2008; 23: 265–73.

Tobimatsu S, Zhang YM, Kato M. Steady-state vibration somatosensory evoked potentials: physiological characteristics and tuning function. Clin Neurophysiol 1999; 110: 1953–8.

Ugawa Y, Hanajima R, Terao Y, Kanazawa I. Exaggerated 16–20 Hz motor cortical oscillation in patients with positive or negative myoclonus. Clin Neurophysiol 2003; 114: 1278–84.

Uhlhaas PJ, Singer W. Neural synchrony in brain disorders: relevance for cognitive dysfunctions and pathophysiology. Neuron 2006; 52: 155–68.

Weinberger M, Mahant N, Hutchison WD, Lozano AM, Moro E, Hodaie M, et al. Beta oscillatory activity in the subthalamic nucleus and its relation to dopaminergic response in Parkinson's disease. J Neurophysiol 2006; 96: 3248–56.

Williams D, Tijssen M, Van Bruggen G, Bosch A, Insola A, Di Lazzaro V, et al. Dopamine-dependent changes in the functional connectivity between basal ganglia and cerebral cortex in humans. Brain 2002; 125: 1558–69.

Witjas T, Regis J, Viallet F, Sethian M, Peragut JC, Azulay JP. Is bilateral stimulation of the subthalamic nucleus less effective in Parkinson's disease when procedure is done under general anesthesia? A prospective study of 75 patients. Mov Disord 2004; 19: S301.

Wojtecki L, Timmermann L, Jörgens S, Südmeyer M, Maarouf M, Treuer H, et al. Frequency-dependent reciprocal modulation of verbal fluency and motor functions in subthalamic deep brain stimulation. Arch Neurol 2006; 63: 1273–76.